DOI: 10.13009/EUCASS2017-416

Aeroshape Trade-Off and Aerodynamic Analysis of the Space-Rider Vehicle

M. Marini, M. Di Clemente*, G. Guidotti*, G. Rufolo*, O. Lambert**, N. Joiner[†], D. Charbonnier[‡], M.V. Pricop[¥], M.G. Cojocaru[¥], D. Pepelea[¥], C. Stoica[¥], A. Denaro[§]*

**CIRA, Italian Aerospace Research Centre*

Via Maiorise, 81043 Capua (CE), Italy

***Dassault Aviation*

78, Quai Marcel Dassault, 92552 St. Cloud Cedex 300, France

[†]Fluid Gravity Engineering Ltd.

1 West Street, Emsworth, PO10 7DX, United Kingdom

[‡]CFS Engineering

EPFL Innovation Park, Building A, CH-1015 Lausanne, Switzerland

[¥]INCAS, National Institute for Aerospace Research "Elie Carafoli"

B-dul Iuliu Maniu 220, sect. 6, Bucharest, 061126, Romania

[§]TAS-I, Thales Alenia Space Italy

Strada Antica di Collegno 253, 10146 Turin, Italy

Abstract
The Space Rider program is the continuation of the IXV experience and it applies all the design, development and flight experiences to an operative vehicle in order to support the innovation of re-entry technologies for reusable systems, and to provide European routine access and return from orbit, with the purpose to perform in-orbit operation, experimentation and demonstration. Such an ambitious goal calls for a robust flying platform with autonomous capabilities during the descent and landing phases. During the phase A of the project, different classes of aeroshape have been proposed and investigated for the trade-off: lifting body, winged body and capsule. Trade-off has relied only on a qualitative evaluation of different aspects (performance, volume, flexibility, development effort), and the IXV-like lifting body concept has been finally selected. The trade-off allowed to down-select two candidate aeroshape configurations, the first being exactly the “IXV 1:1” and the second being a variant of IXV with addition of vertical fins, for which an extensive aerodynamic investigation has been defined and put in place, both at numerical (Phases A and B1) and experimental (Phase B1) levels. The paper reports in detail all the aerodynamic results on the two configurations.

Nomenclature

AEDB	Aerodynamic Data Base	LCDP	Lateral Control Departure Parameter
AoA	Angle of Attack (also α)	L/D	Aerodynamic Efficiency
AoS	Angle of Sideslip (also β)	L_{ref}	Reference Length
ATDB	Aerothermodynamic Data Base	M	Mach number
CFD	Computational Fluid Dynamics	MCI	Mass, Centre of Gravity, Inertia
C_A	Axial force coefficient	MRC	Moment Reference Centre
C_D	Drag coefficient	P_0	Reservoir (stagnation) pressure
C_L	Lift coefficient	p, q, r	Roll, pitch, yaw rates
C_l	Rolling moment coefficient (also C_{ll})	RANS	Reynolds-Averaged Navier Stokes
C_m	Pitching moment coefficient	RCS	Reaction Control System
C_N	Normal force coefficient	S_{ref}	Reference Surface
C_n	Yawing moment coefficient (also C_{ln})	T_0	Reservoir (stagnation) temperature
C_Y	Side force coefficient	TPS	Thermal Protection System
CoG	Centre of Gravity	V	Velocity
FQ	Flying Qualities	WB	Winged Body
IXV	Intermediate eXperimental Vehicle	WTT	Wind Tunnel Test
LB	Lifting Body	δ_e, δ_a	Elevon, aileron deflection

DOI: 10.13009/EUCASS2017-416

1. The Space Rider Program

The Space-Rider Program [1] overall objective is to develop an affordable reusable European space transportation system to be launched by VEGA-C, and to perform experimentation and demonstration of multiple space application missions in Low Earth Orbit (see Figure 1).
The program hints are: to perform application-driven missions with a payload mass capability up to 800 kg for a multitude of orbits altitudes and inclinations; to benefit at the maximum extent possible from existing launchers technologies; and, to address relevant progressive technological challenges with limited risks and minimal financial efforts for Europe.
Therefore, in line with the above guidelines, the Space-Rider shall provide routine access to and return from orbit, with the purpose to perform in-orbit operation, experimentation and demonstration for the following applications: Free-Flyer applications, In-Orbit Demonstrations and Validation for the following technologies, and In-Orbit applications.
The Program has successfully passed the Phase A critical milestone, the Preliminary Requirements Review (PRR), and is currently in the Phase B1 targeting the final review of this stage, the System Requirements Review (SRR).

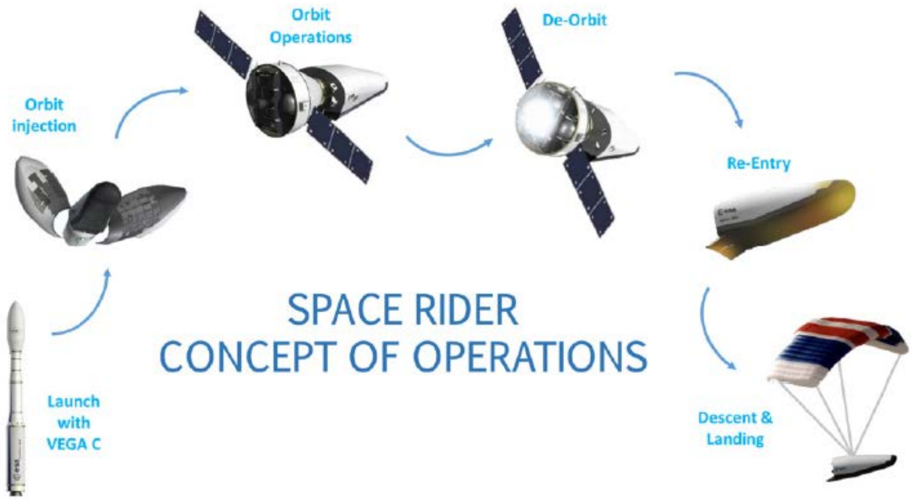

Figure 1: Space-Rider concept of operations

2. Aeroshape Class Selection

The Space-Rider baseline aeroshape has been selected in two phases: 1) selection of the most appropriate aeroshape class among different classes; 2) within the selected class analysis of alternative aeroshape configurations and selection of the baseline.

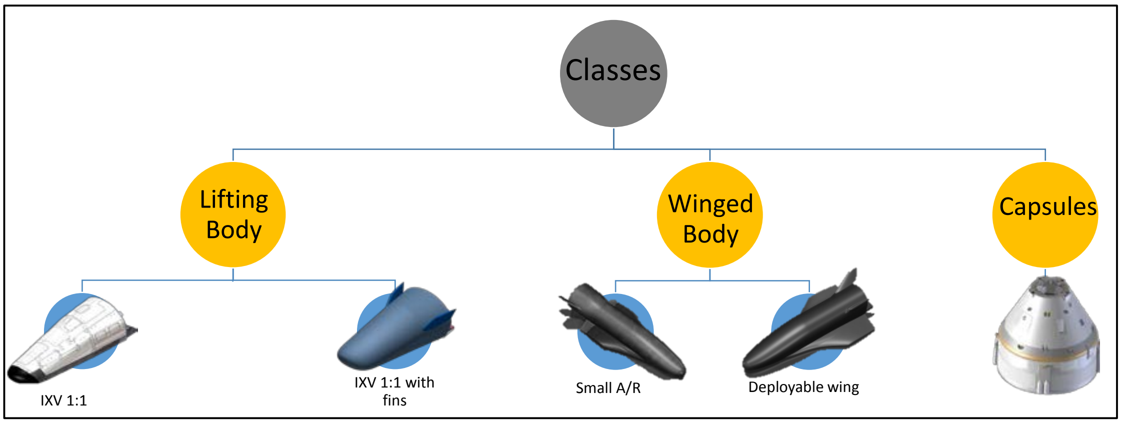

Figure 2: Space-Rider aeroshape classes for selection

The selection of the most appropriate class of aeroshape has been carried out following the standard step-wise process by using multi-criteria decision analysis based on definition of criteria and identification of alternatives. Criteria have

DOI: 10.13009/EUCASS2017-416

been assigned a weight, and the evaluation of alternatives, either by technical analysis or by qualitative judgment, has been done by assigning a fulfilment grade w.r.t. each single criterion. Finally, the ranking of alternatives has led to down-selection of the best solution.
The classes of shapes investigated for the trade-off have been three: Lifting Body (LB), Winged body (WB), and Capsules (see Figure 2). The adopted high-level criteria for the evaluation have been defined based on programmatic and system-level needs as follows:

- System architecture performance (C1)
  - Rationale: the criterion is to be intended as need for maximization of fly-ability (capability to cover the wide flight envelope from re-entry down to landing).
  - Factor/Parameter: the parameter based on which the alternative is evaluated against the criterion is the stability/maneuverability (down to regimes compatible with state-of-art parafoil technology).
- Volume figure (C2)
  - Rationale: the criterion is to be intended as the need to choose a shape class that enables maximization of payload mass/volume.
  - Factor/Parameter: the parameter based on which the alternative is evaluated against the criterion is the shape volume occupation in VEGA/volume available for payload.
- Configuration flexibility / compatibility (C3)
  - Rationale: the criterion is to be intended as the need to choose a shape class that enables maximization of compatibility with VEGA.
  - Factor/Parameter: the parameter based on which the alternative is evaluated against the criterion is in this case the shape interference with VEGA fairing, CoG and static unbalance, natural frequencies.
- TRL for the PRIDE and Development Effort (C4)
  - Rationale: the criterion is to be intended as the need to choose a shape class that enables minimization of development effort.
  - Factor/Parameter: the parameter based on which the alternative is evaluated against the criterion is in this case the aerodynamic/aerothermodynamic characterization, TPS solutions, Control Surfaces, etc. Satisfaction level is judged in terms of delta-effort to be put in place with respect to already inherited from IXV project. Three levels of impact have been adopted: Green for No or Low Δ-design; Yellow for Moderate Δ-design; Red for High Δ-design.

Table 1: Alternatives' Scale of Satisfaction

Qualitative grade	**Very good**	**Good**	**Fairly good**	**Poor**	**Very poor**
Absolute grade	5	4	3	2	1

For the sake of simplicity, criteria are assigned the same level of importance, then the same weight. While, as far as alternatives are concerned, a scale of satisfaction was defined based on five levels, defined as absolute or qualitative, and each of them is then assigned a numerical value accordingly (see Table 1).
Trade-off results are reported from Figure 3 to Figure 7. The most promising class of shape is the Lifting Body as shown in Table 2.

	C1	**Lifting Body**	**Winged Body**	**Capsules**
Evaluation	Rationale	(typ. L/D 0.7) Lifting Body can ensure a fairly good capability to manage the flying part of the mission from re-entry down to regimes compatible with parafoil systems [10÷8km of altitude; Mach 0.8÷]	(typ..: L/D 1.0) w.r.t. maneuverability from reentry down to sea level, winged vehicles are the most promising alternative because of their intrinsic added value: the combination of RCS during re-entry and of wing, fins, and control surfaces (rudders, ailerons/elevens, body flaps) provide the system with a great capability in terms of down/cross-range and precision landing.	(typ. L/D <0.3) Although an enhanced RCS could provide a certain degree of maneuverability during reentry and atmospheric flight at very high altitudes, capsules are rather semi-ballistic systems with very limited flexibility w.r.t. what we need in Space Rider (great cross-range and high precision landing)
	Grade	Good	Very good	Very Poor

Figure 3: Aeroshape alternatives evaluation against criterion C1

DOI: 10.13009/EUCASS2017-416

C2 (a)		Lifting Body	Winged Body	Capsules
Evaluation	Rationale	IXV-like shape builds upon the X-38 shape with the rational to fill the empty (unexploited) volume between the vertical fins and the leeward side of the fuse: hence LB is a good compromise that can ensure a good exploitation of the volume under the fairing.	In terms of volume efficiency the winged vehicles are probably the most penalizing alternative because their shape claims for slender shape factor (or at least the shape builds on the combination of a fuse + a wing, and the wing is a part of the system that cannot be used to host P/L or equipment): this does not allow to exploit the faring volume at the best. Deployable wing version can solve the problem but at a great pay-off in terms of complexity as well as mass for mechanisms.	Being axis-symmetric bodies, the capsules can be shaped in such a way to maximize exploitation of fairing envelope. But fill all the available volume under a fairing is not always the best choice because a greater capsule reuires a heavier CS and TPS, then mass and CoG issues can arise form that approach.
	Grade	Very Good	Poor	Good

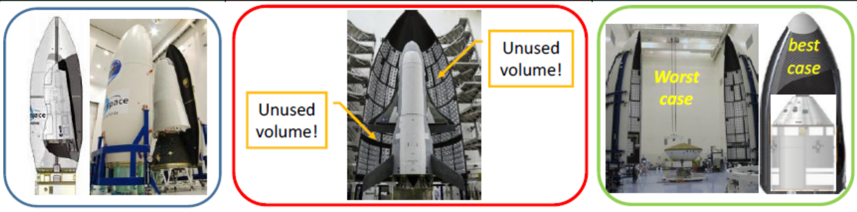

Figure 4: Aeroshape alternatives evaluation against criterion C2, part A

C2 (b)		Lifting Body	Winged Body	Capsules
Evaluation	Rationale	w.r.t. the Space Rider application the LB requires implementation of system resources manageable exploiting the IXV design at maximum extent with a delta-implementation due to orbital and landing phases. Provided that the orbital phase is common to all the options, the landing phase requires a Landing System which replaces the IXV Recovery System. The landing being classified as "soft" might not imply the same complexity as in the wheeled LS necessary for a WB. In synthesis, LB needs resources in an amount and complexity much lower than WB and similar to Capsules.	A WB inevitably asks for a larger set of system resources in order to cover the functions to be preformed: nominally wings, flaps and fins are exposed areas to be protected (and they do not offer volume for equipment allocation), hence they represent a penalty in terms of cold structure, TPS, actuators and relevant avionics. Moreover, high speed landing system introduces additional penalty due to wheels and brakes (which are not required for a soft-landing as in LB/Capsules options). Hence, being fixed the whole system mass at launch (2575kg), all these additional system resources represent a mass/volume pay-off for the payloads.	In terms of system-resources capsules are much simpler than WB and slightly simpler than LB. Nevertheless, reusability implies inevitably design choices that lead to mass and volume penalties: a reusable capsule shall feature a robust CS (then heavier) because the re-entry and landing loads are higher than LB and WB. Ablative heat shield can be implemented but this is not reusable: if we go for reusable TPS on capsule would require a much greater thickness or a different technology (which implies a greater impact for integration on the system) Descent system shall be also robust to decelerate enough the vehicle: alternative ways might be retro-rockets which imply a pay-off again. A landing system shall be also implemented in order to cope with the landing: either a conventional option (legs) or less-conventional one (air-bag) would imply a pay-off.
	Grade	Good	Very poor	Good

Figure 5: Aeroshape alternatives evaluation against criterion C2, part B

C3		Lifting Body	Winged Body	Capsules
Evaluation	Rationale	• IXV heritage proves that a good compatibility is reachable with appropriate design choices.	• Being slender body, a WB features in principle low bending frequencies and higher CoG position w.r.t. separation plane. • Being non axis-symmetric, it features a Z CoG position out of the LV axis. • Wings and fins must be sized to lay inside the fairing envelope which implies a small size of the whole vehicle: deployable wing version can solve the problem but at a great pay-off in terms of complexity and mass.	• Being axis-symmetric bodies, the capsules can be shaped in such a way lay inside the fairing envelope and to feature enough area on the rear plate to fit with the LV adapter. • however in case the capsule shape fill all the available volume then there will be a problem of CoG too high w.r.t. separation plane. For this reason capsule are better than WB but worse than LB
	Grade	Good	Poor	Good

Figure 6: Aeroshape alternatives evaluation against criterion C3

3. Baseline Aeroshape Identification

Within the best class of shape, the Lifting Body, a further trade-off has been carried out with respect to the most promising aeroshape. For that purpose, two different shapes have been considered and evaluated, see Figure 8.
The first one is the "IXV 1:1", which is deemed a very good candidate as it has successfully flown down to low supersonic regime. Nevertheless, it has to be verified its fly-ability down to transonic and subsonic regime in order to be fully eligible for the Space-Rider mission. The second one is the "IXV 1:1 with Fins", a variant of IXV that can

DOI: 10.13009/EUCASS2017-416

perform as IXV in the hypersonic and supersonic regimes, while it might also provide aerodynamic performance improvement in the transonic and subsonic regimes.

		Lifting Body	Winged Body	Capsules
Sys.Design	AED, ATD	Minor delta due to winglets	Significant delta due to New AEDB &ATDB	Moderate delta due to New AEDB&ATDB
	Mission Analysis	Orbital/Landing phases are a novelty but do not introduce great challenges	Significant delta: all phases to be designed	Significant delta: all phases to be designed
	GNC	Orbital + Parafoil Flight	Significant delta: all phases to be designed	GN&C is simpler than WB/LB but in case of retro-rokets is a challenge
Sub-System Technologies	Cold Structure	Landing loads introduce delta-design	Completely different from IXV	New design but simpler than WB
	Mechanisms	Cargo Bay Doors, Solar Arrays, LG doors do not appear critical	LB + Wing Deployment Sys	Similar complexity to LB
	Descent & Landing System	Parafoil + LS are worth of moderate delta-design but manageable	High-speed Landing Gear is a challenge	Significant delta for DLS + Retrorockets are necessary for soft-landing and reusability
	TPS &HS	Low delta-design to put in place for refurbishment	Wings L.E. + Deployable Sys Rudders\Fins are a challenge	Ablative shield to be developed
	TCS/ECS	An equivalent not-negligible design effort is expected for the 3 options for all phases		
	Avionics	An equivalent design effort is expected for the 3 options for orbital phase (Rad-hard, ruggedized and compact solutions are necessary)		
	ASCS	Parafoil Control is a delta but moderate	Wing + Tail ASCS is a challenge	Not applciable
	RCS/OMS	OMS is a moderate delta	OMS/RCS similar to IXV/LB	Retro-rocket for Landing is a challenge
Fulfillment grade		Good	Very poor	Poor

Figure 7: Aeroshape alternatives evaluation against criterion C4

Table 2: Class Alternatives evaluation and final ranking

criteria	weight	Lifting body	Winged body	Capsule
C1	0.25	Good	Very good	Very poor
C2a	0.125	Very good	Poor	Good
C2b	0.125	Good	Very poor	Good
C3	0.25	Good	Poor	Good
C4	0.25	Good	Very poor	Poor
Final ranking		1°	3°	2°

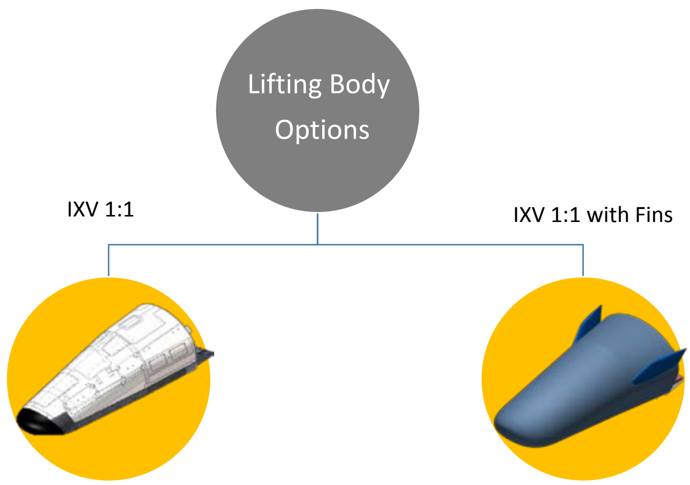

Figure 8: Lifting body shapes alternatives

DOI: 10.13009/EUCASS2017-416

A simplified analysis of advantages and drawbacks of the two configurations is summarized in Table 3.
It is remarked that the "IXV 1:1" aeroshape is a very good candidate because it allows maximization of IXV heritage from any perspective and it ensures the extension of fly-ability envelope down to transonic/subsonic regime within a given set of assumptions (e.g., AEDB, MCI and AoA uncertainties). The fly-ability verification has to be completed with the support of further Flight Quality investigation.
The "IXV with Fins" is on one hand a promising variant as long as a maximization of the vehicle down-range and cross-range capability, and lateral-directional static and dynamic stability, are concerned, however fins imply a pay-off of mass, structural modifications and a delta-characterization in terms of aerodynamics and aerothermodynamics. Hence, the pay-off that the shape introduces seems to be more significant than the advantages.

Table 3: Pros and Cons of IXV shape and its variants

shape	Pros	Cons	Score
IXV 1:1	• Full exploitability of IXV heritage and data (AED/ATD) • stability and controllability in longitudinal and lateral down to Mach 0.6 following a natural trim at high AoA (TBC) • No impact on the system compared to the fins version	• FQ investigation to be completed	Very good
IXV 1:1 with fins	• Large Cm curve shift-down in both AoS=0° and AoS=5° • Natural trim achieved at lower AoA (higher L/D), or reduced de need for trim • Lateral-directional static and dynamic behavior clearly improved especially at lower Mach (0.6) and lower AoA	• Need for TPS on fins implies a pay-off of mass as well as complexity of the system • Need for negative δ_e to trim at supersonic/hypersonic Mach numbers	Good

For all the reasons discussed above:

- the "IXV 1:1" aeroshape is considered the baseline for the Space-Rider project even though delta-investigations are necessary to fully award this shape as the best candidate to fulfil the fly-ability need;
- The "IXV with Fins" aeroshape is kept as optional, in the sense that additional analyses are necessary to verify whether or not the fins might provide a significant advantage from a fly-ability standpoint.

Then, the aerodynamic activities have been developed with the characterization in the transonic-subsonic regime by CFD and WTT of the IXV aeroshape (without and with fins).

4. Aerodynamic Analysis of the Space Rider Vehicle

The "IXV 1:1" aerodynamic database [2], valid down to M=1.2, has been extended through new numerical computations and available experimental data (from IXV project) down to Mach=0.6, in order to assess IXV flying qualities when passing through this flight domain, and assuming that the internal layout of the vehicle can be adapted to recover IXV's CoG location that is compatible with aerodynamic behavior.
The "IXV 1:1 with Fins" option has also been investigated through numerical computations, in order to evaluate the strategy to pass through transonic regime at a lower angle of attack and, therefore, higher aerodynamic efficiency, and with an improved lateral-directional stability. The candidate solution to achieve the goals above has been identified in adding a couple of vertical fins mounted on aeroshape leeside, which have been properly shaped and sized. This configuration has been analyzed through CFD computations at different Mach numbers in order to derive an updated version of the aerodynamic database.
In the following paragraphs, all the steps of these aerodynamic database setups are reported, together with a comparative aerodynamic analysis of both configurations. Details about the sizing of vertical fins are also given.

4.1 Aerodynamic Data Base Development and Aerodynamic Analysis

CFD Simulations

The Space-Rider CFD Repository has been organized and managed with the same rules and standards used to organize the previous IXV CFD Repository. The Phase-A Space-Rider CFD Repository contains CFD simulation results delivered by the following project partners:

- CIRA for both configurations ("IXV 1:1" or "IXV as it is" and "IXV with fins")
- Fluid Gravity Engineering Ltd. (FGE) for both configurations ("IXV 1:1" and "IXV with fins")
- CFS Engineering (CFSe) for both configurations ("IXV 1:1" and "IXV with fins")

DOI: 10.13009/EUCASS2017-416

- Dassault-Aviation (DAA) for the configuration “IXV 1:1” (both aeroshape 2.2 and 2.3)

CFD results for the aeroshape IXV with fins refer to the last fin configuration (i.e., “FIN03-B”), the result of a trade-off study performed by CIRA from the Kick-Off meeting of the project to the Progress Meeting PM1, as it will be detailed in the following.

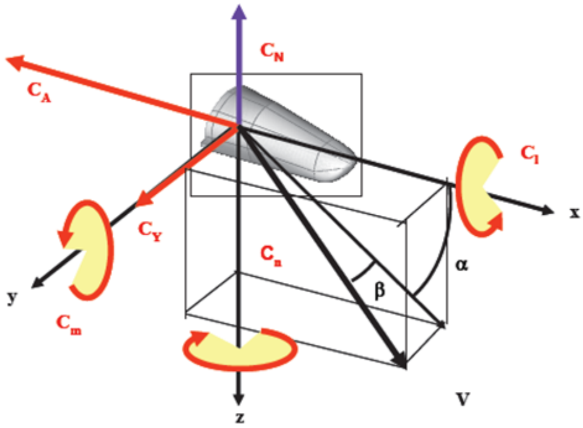

Figure 9: Aerodynamic convention

Aerodynamic conventions and signs of aerodynamic coefficients (C_N, C_A, C_Y, C_{ll}, C_m, C_{ln}) are indicated in Figure 9. The reference length is L_{ref}=4.4m, the reference surface is S_{ref}=7.26 m^2, while the moment reference center (MRC) is located in the plane of symmetry at 58% of the reference length from the nose, i.e. MRC=[1.848, 0.0, 0.11] m in the adopted coordinate system.
The CFD test matrices are reported in the following tables, for what concerns both the aeroshape “IXV as it is” (CFD simulations by Dassault-Aviation, see Table 4, a total of 108 half-body equivalent CFD simulations considering the ones for aeroshape 2.2 and aeroshape 2.3) and the “IXV with fins”, named “FIN03-B” (CFD simulations by CIRA, FGE, CFSe, see Table 5, a total of 80 half-body equivalent CFD simulations).

Table 4: CFD matrix for “IXV as it is” aeroshapes 2.2 and 2.3 (DAA)

					Mach	0.6	0.8	0.95	1.2
Theme	Alfa (°)	Beta (°)	DE (°)	DA (°)	Z (km)	13.4	20	23.8	27.6
Clean Longitudinal	35	0	0	0		X	X	X	X
	45					X	X	X	X
	55					X	X	X	X
	65					X	X	X	X
Longi. flap efficiency	35	0	-5	0			X		
			5				X		
			10				X		
	55	0	-5	0			X		
			5				X		
			10				X		
Clean Lateral	35	5	0	0		X	X	X	X
	45					X	X	X	X
	55					X	X	X	X
	65					X	X	X	X

The reference free-stream conditions used for the CFD simulations of Table 4, dedicated to assess the effect of aeroshape 2.3 vs. 2.2 with regard to FOI/STARCS T1500 WTT data [3][4][5], have been the following: Mach numbers 0.6, 0.8, 0.95 and 1.20, respectively at the altitudes of 13.4, 20, 23.8 and 27.6 km. In particular, with these CFD simulations the longitudinal aerodynamics in clean configuration and flapped configuration, and the sideslip effects (AoS=5 deg) in clean configuration, have been studied.
The freestream conditions used for the simulations of Table 5 have been extracted by the REF-D2 IXV nominal trimmed trajectory, where flight conditions for the transonic and subsonic phase have been preliminarily assumed. As wall thermal conditions, adiabatic wall has been assumed up to Mach=2 condition and radiative equilibrium (with emissivity coefficient ε=0.8) from Mach=4 to Mach=25. For reacting flows computations, the wall has been considered as fully catalytic.

DOI: 10.13009/EUCASS2017-416

Table 5: CFD matrix for aeroshape "IXV with Fins" (CIRA, FGE, CFSe)

Mach	alt (km)	AoA	AoS	flow modelling	provider	FIN03-B	IXV	TOTAL
0,6	12	50	0	ideal gas, turbulent	CIRA	1	1	2
0,6	12	55	0	ideal gas, turbulent	CIRA	1	1	2
0,6	12	60	0	ideal gas, turbulent	CIRA	1	1	2
0,6	12	65	0	ideal gas, turbulent	CIRA	1	1	2
0,6	12	55	5	ideal gas, turbulent	CIRA	2	2	4
0,6	12	65	5	ideal gas, turbulent	CIRA	2	2	4
0,8	12	20	0	ideal gas, turbulent	CIRA	1	1	2
0,8	12	30	0	ideal gas, turbulent	CIRA	1	1	2
0,8	12	45	0	ideal gas, turbulent	CIRA	1	1	2
0,8	12	55	0	ideal gas, turbulent	CIRA	1	1	2
0,8	12	45	5	ideal gas, turbulent	CIRA	2	2	4
0,8	12	55	5	ideal gas, turbulent	CIRA	2	2	4
0,95	18	35	0	ideal gas, turbulent	CIRA	1	1	2
0,95	18	40	0	ideal gas, turbulent	CIRA	1	1	2
0,95	18	45	0	ideal gas, turbulent	CIRA	1	1	2
0,95	18	50	0	ideal gas, turbulent	CIRA	1	1	2
0,95	18	45	5	ideal gas, turbulent	CIRA	2	2	4
0,95	18	50	5	ideal gas, turbulent	CIRA	2	2	4
1,2	24,74	40	0	ideal gas, turbulent	CIRA	1	1	2
1,2	24,74	50	0	ideal gas, turbulent	CIRA	1	1	2
1,2	24,74	55	0	ideal gas, turbulent	CIRA	1	1	2
1,4	25,51	35	0	ideal gas, turbulent	CIRA	1	1	2
1,4	25,51	45	0	ideal gas, turbulent	CIRA	1	1	2
1,4	25,51	55	0	ideal gas, turbulent	CIRA	1	1	2
1,7	26,77	35	0	ideal gas, turbulent	FGE	1	1	2
1,7	26,77	45	0	ideal gas, turbulent	FGE	1	1	2
1,7	26,77	55	0	ideal gas, turbulent	FGE	1	1	2
2,0	28,36	45	0	ideal gas, turbulent	FGE	1	1	2
4,0	37,39	45	0	ideal gas, turbulent	FGE	1	1	2
6,0	43,31	45	0	ideal gas, turbulent	FGE	1	1	2
10,00	52,11	45	0	eq, turbulent	CFSe	1	avail CFSe	1
10,00	52,11	45	0	eq, laminar	CFSe	1	avail CFSe	1
17,70	64,58	45	0	noneq, laminar	CFSe	1	avail CFSe	1
25,00	76,54	45	0	noneq, laminar	CFSe	1	1	2

Note that in the case of aeroshape with fins only simulations in clean configuration (δ_e=δ_a=0 deg) have been performed, in the hypothesis of using the same aileron/elevon efficiency of the IXV aeroshape as it is. In the AEDB generation for the aeroshape configuration with fins, the same has been assumed for the aerodynamic uncertainties and the damping derivatives (C_{mq}, C_{lp}, C_{lr}, C_{np}, C_{nr}).
A Space-Rider CFD Repository Database (vs. 1.0) has been prepared by CIRA collecting all CFD results of CIRA, FGE, CFSe and DAA on both aeroshape configurations. Standards for CFD simulations' outputs have been defined and properly applied.
As far as CFD codes are concerned, CIRA have used their code ZEN [6] which solves the RANS equations in the frame of a finite volume approach on structured multi-block grids. The k-ω TNT two-equation turbulence model has been employed in the hypothesis of fully turbulent flow. Working gas is air considered as an ideal gas in the flight conditions investigated. The computational grids were generated by the ANSYS ICEMCFD software package. Typically, a half-body configuration was composed by 3.5÷4 million cells, while a full configuration is composed by 7.5÷8.8 million cells. Some exemplary results are shown in Figure 10.
FGE have used their in-house ANITA code and unstructured grids for their supersonic and cold hypersonic simulations by using an ideal gas model, with viscosity computed from Sutherland's expression for air and thermal conductivity determined using a constant Prandtl number of 0.7 and heat capacity c_p=1003.747 J/kg/K. The thermal boundary condition for cases with M>2 is radiative equilibrium (with emissivity of 0.8), all other points are adiabatic. The inviscid flux numerical modelling has been adapted to the particular case, while SST turbulence model has been employed in all simulations.
CFSe have used their NSMB flow solver [7] which uses a cell centered finite volume method to solve the compressible RANS equations, and ANSYS ICEMCFD pre-processer to generate the multi-block structured grid. The blocking and the mesh have been generated in order to optimally use the bow shock adaption procedure available within the solver. All the calculations have been carried out with a second order central spatial scheme, i.e. second order TVD-type numerical dissipation terms were added to the central space discretization to prevent numerical oscillations. The governing equations have been integrated in time using the LU-SGS implicit scheme. Both equilibrium and non-equilibrium flow computations have been performed, and when the flow is considered turbulent, the Wilcox k−ω turbulence model has been used.

DOI: 10.13009/EUCASS2017-416

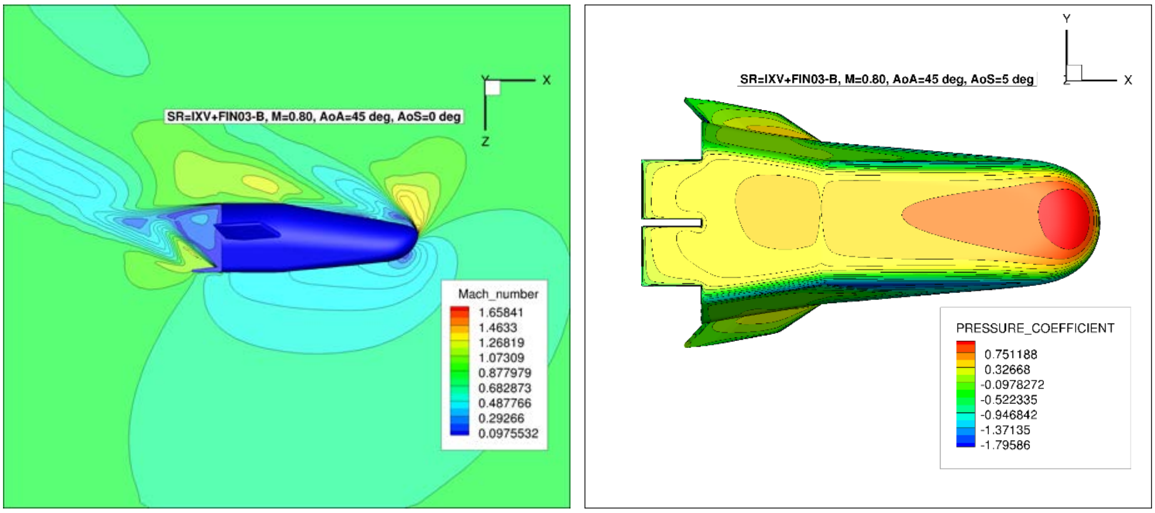

Figure 10: exemplary CFD results for aeroshape “IXV with fins”, Mach=0.8, AoA=45 deg, AoS=5 deg

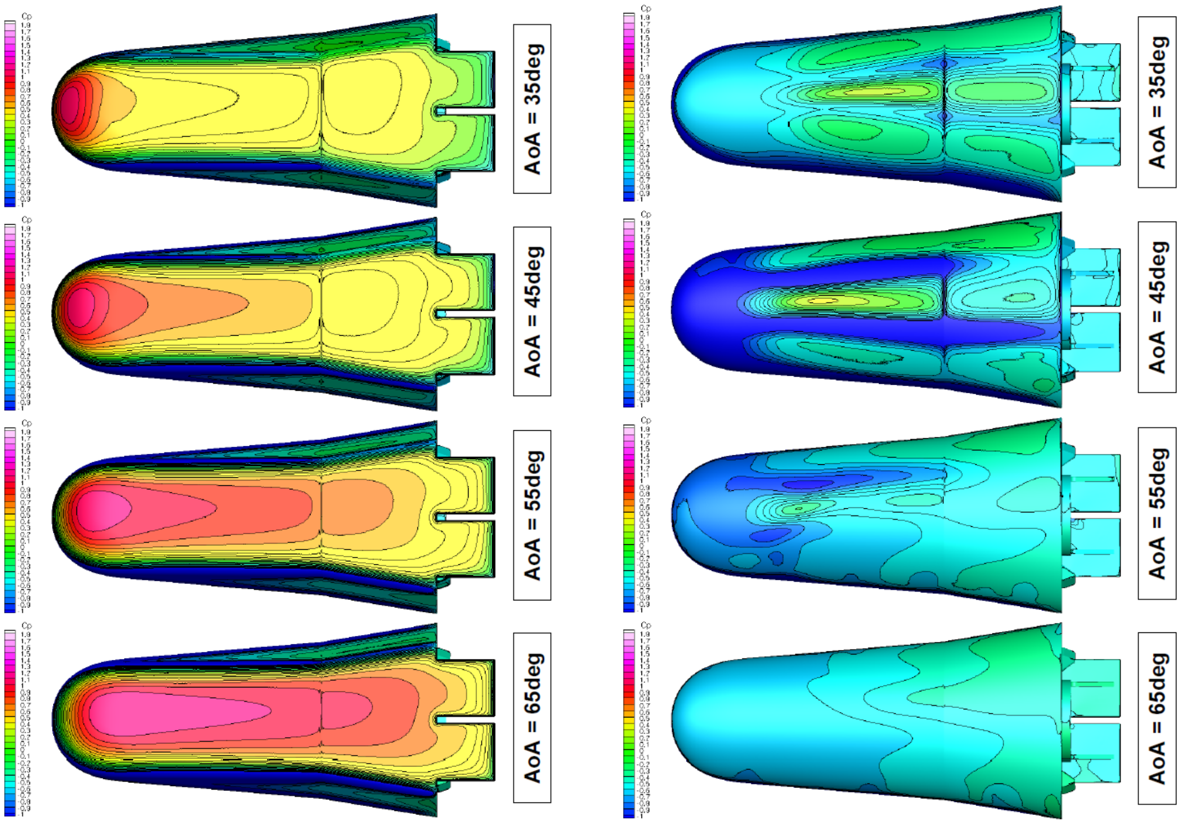

Figure 11: exemplary CFD results for aeroshape “IXV 1:1”, Aeroshape 2.3, C_p distribution, Mach=0.6, AoS=-5 deg

Dassault-Aviation have performed the simulations by using the CFD code AeTher [8], with a two-layers k-ε turbulence modelling. IXV aeroshape versions 2.2 and 2.3 both include the launcher ring adaptor and the four RCS pods at the base of the vehicle, the only difference between these two shapes being the shape of the body flaps: rectangular profile for aeroshape 2.2, trapezoidal (tapered) profile with curvature radiuses at the trailing edge for aeroshape 2.3 with a rod stiffener at the leeward side of the flap. Surface and volume non-structured meshes have been generated with DAA in-house meshing tools.
Some results produced by Dassault-Aviation are shown in Figure 11.

DOI: 10.13009/EUCASS2017-416

Optional Aeroshape: IXV with fins

Regarding the Space-Rider aeroshape identification, a strategy to pass through transonic regime at lower AoA and higher aerodynamic efficiency has been investigated at the beginning of Phase A. The available IXV aerodynamic data in subsonic and transonic regime, i.e. the FOI/STARCS T1500 WTT experimental results [3], [4], [5] and the AEDB_5.1.4 [2], were reviewed and some major issues were identified: the aeroshape as it is can fly only following natural trim (high AoA, up to about 70 deg) down to M=0.60 since flap efficiency reduces drastically; further, some lateral instabilities ($C_{n\beta}$, $C_{Y\beta}$) occur at M=0.60 and lower AoA (where the vehicle is longitudinally stable, of course).
To solve these problems, different vertical fins were shaped and sized with engineering methods [9][10][11], and a trade-off study was performed to conciliate their aerodynamic effectiveness (shift down of C_m curves, sign inversion of $C_{n\beta}$) and their structural feasibility (interference with the VEGA-C fairing dynamic envelope, need for TPS, etc.).
The aerodynamic performance of the final version of the fin (named “FIN03-B”), smaller and with lower impact on weight and structures, was predicted by means of 80 CFD half-body equivalent simulations (ideal gas, turbulent flow), defined in agreement with DAA (complete Mach number coverage, AoA sweeps and AoS sweeps in subsonics and transonics, both configurations: IXV as it is and IXV+FIN03-B, see Figure 12), to be computed in such a way to allow Dassault-Aviation to prepare the AEDB for this new configuration. A preliminary FQ analysis was also performed in terms of C_m curve shift-down, lateral-directional derivatives, $C_{n\beta,dyn}$ and LCDP.

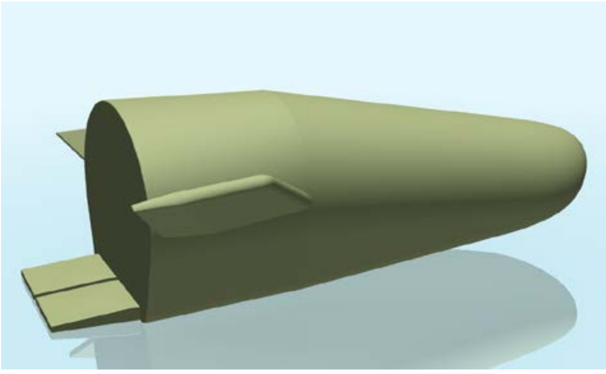

Figure 12: Space-Rider aeroshape with vertical fins FIN03-B

FIN03-B is characterized by an outboard surface of 0.58 m^2, an inboard surface of 0.40 m^2, a root chord of 1.23 m, a tip chord of 1.10 m and a fin’s height at trailing edge of 0.48 m. Fin’s leading edge is swept back of 54 deg whereas its trailing edge of 51 deg, while the angle formed by the fin plane and the symmetry plane of the aeroshape is 49 deg at leading edge and 44 deg at trailing edge. Furthermore, the fin tip has been properly rounded.
The vertical fin FIN03-B implemented on the Space-Rider vehicle has worked as expected, being characterized by:

- large C_m curve shift-down, also with a sideslip angle;
- natural trim achieved at lower AoA (i.e. slightly higher L/D), or reduced δ_e needed for trim at lower AoA;
- need for large negative δ_e to trim the vehicle at supersonic and hypersonic Mach numbers;
- lateral-directional aerodynamics confirmed (C_l<0) or clearly improved (C_Y and C_n), especially at lower Mach and AoA (sign inversion of $C_{Y\beta}$ and $C_{n\beta}$ at M=0.60);
- improvement of $C_{n\beta,dyn}$ (no critical effect of I_{zz}/I_{xx}) and LCDP (roll reversal at M=0.6 inhibited).

Some CFD results about the IXV with Fins (FIN03-B) aeroshape, in clean configuration, are shown in Figure 13, Figure 14 and Figure 15.

DOI: 10.13009/EUCASS2017-416

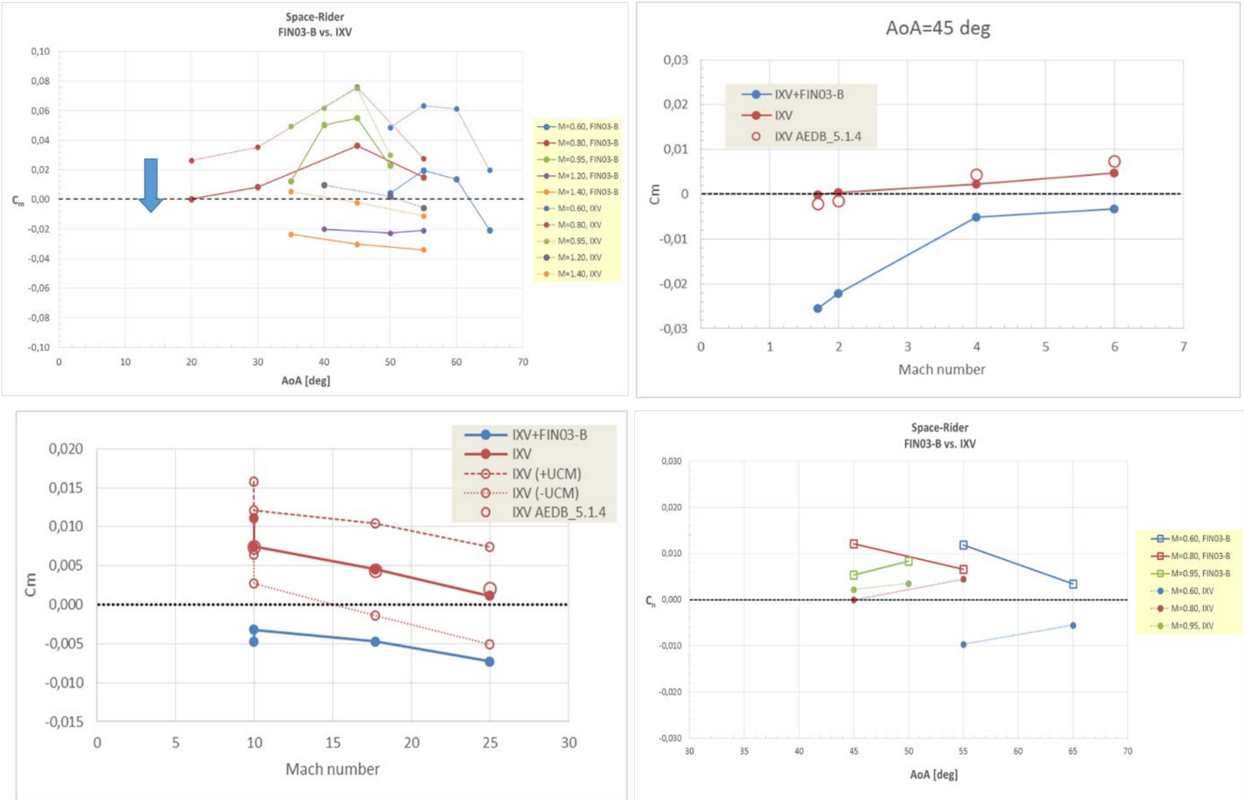

Figure 13: main aerodynamic results of Space-Rider aeroshape with fins (FIN03-B). Pitching moment evolution (top, left); pitching moment evolution at Mach=1.7, 2, 4, 6 and AoA=45 deg (top, right); pitching moment evolution at Mach=10, 17.75, 25 and AoA=45 deg (bottom, left); yawing moment coefficient evolution at at M=0.6, 0.8, 0.95 and AoS=5 deg (bottom, right)

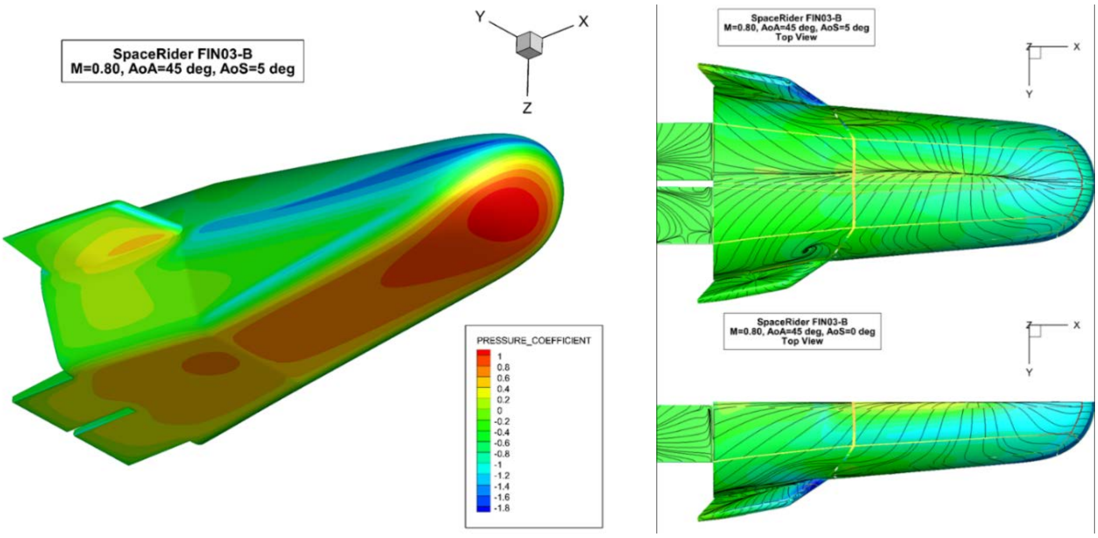

Figure 14: aeroshape with fins (FIN03-B), M=0.80, AoA=45 deg, AoS=5 deg. Pressure contours (left) and skin-friction lines (right)

DOI: 10.13009/EUCASS2017-416

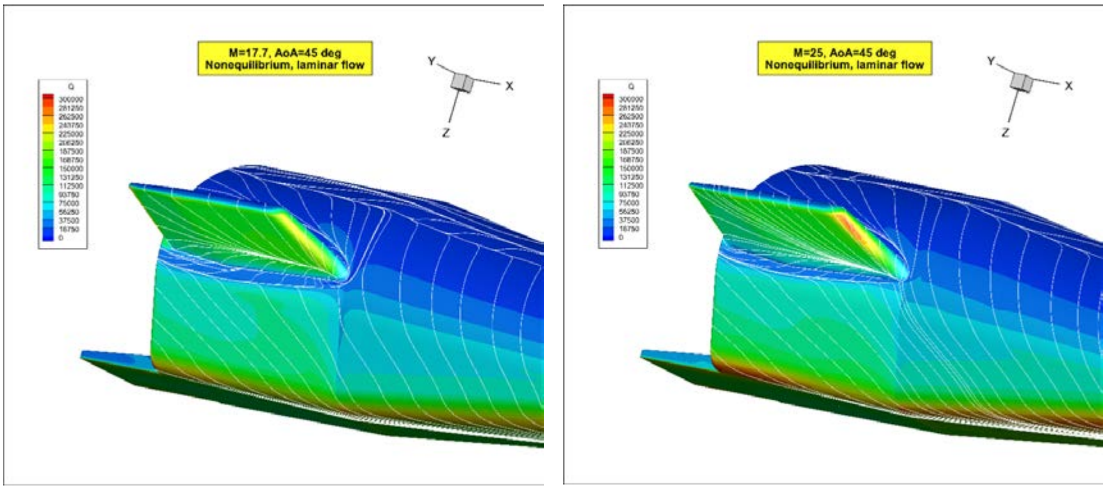

Figure 15: aeroshape with fins (FIN03-B), aerothermal environment at Mach=17.75 (left) and Mach=25 (right)

Development of the Aerodynamic Data Bases

The current Space-Rider Aerodynamic Data Base (AEDB) described hereinafter is composed by two different parts:

- AEDB v6.0 for "IXV 1:1" aeroshape (the baseline) aimed to extend IXV database AEDB v5.1.4 ([2], valid down to M=1.2) to transonic-subsonic regime down to M=0.6, and referred to aeroshape 2.3;
- AEDB v6.0 for "IXV+Fins" aeroshape (the optional) which is identical to IXV AEDB v6.0 (same aileron/elevon efficiency, same uncertainties, same damping derivatives) considering an aeroshape effect between IXV 2.3 and IXV+Fins configuration for clean longitudinal aerodynamics and AoS effect.

These two AEDBs will permit to assess Space-Rider FQ when passing through the transonic-subsonic flight domain for both configurations and approaches. These two AEDBs have been updated basing on numerical activities carried out by different partners in Phase A, and experimental results gathered during the FOI/STARCS WTT campaigns [3][4][5] carried out during IXV project.
The range of validity of both databases is: Mach number ∈ [0.6 ; 30], AoA ∈ [30° ; 70°], AoS ∈ [-5° ; +5°], δ_e ∈ [-15° ; +15°] and δ_a ∈ [-10° ; +10°].
The detailed AEDB formulation for the longitudinal and the lateral-directional aerodynamic coefficients (C_A, C_N, C_m, C_Y, C_l, C_n), and for damping derivatives (C_{mq}, C_{lp}, C_{np}, C_{lr} and C_{nr}), aerodynamic uncertainties, rarefied gas effects, bridging functions and real gas effects is fully reported in Ref. [2]. By supposing that each contribution to the single global coefficient is treated independently from the others, each aerodynamic coefficient is described by a linear summation over a certain number of incremental contributions, following the so-called build-up approach. Of course, some simplifying hypotheses on the different coupling effects have been made basing on previous expertise.

Aerodynamic Analysis: Baseline IXV aeroshape vs Optional IXV with fins

The comparative aerodynamic analysis reported in the following gives an overview of aerodynamic performance and Flying Qualities of the "IXV 1:1" aeroshape and the "IXV with Fins" aeroshape (with CoG=MRC) in transonic and subsonic regimes extracted from their related AEDBs v6.0.

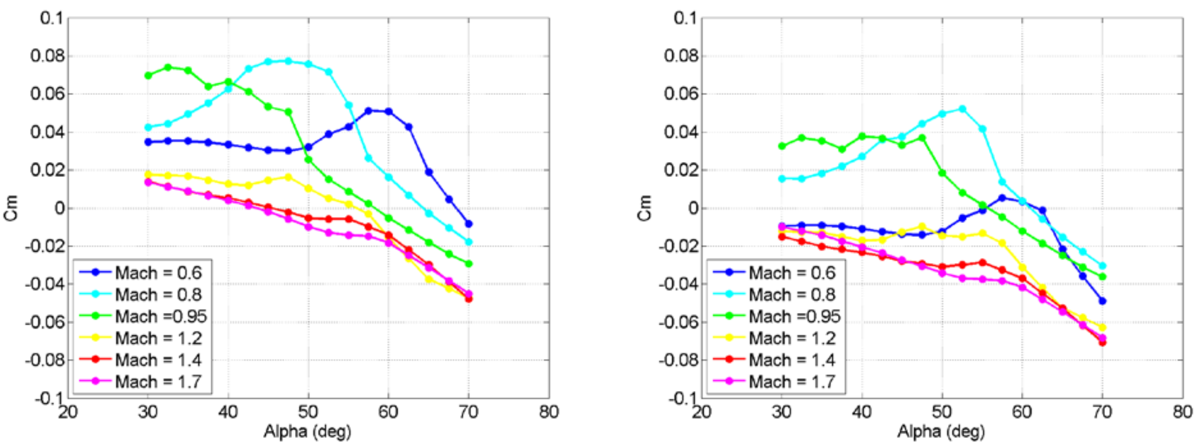

Figure 16: pitching moment coefficient for IXV configuration (left) and IXV+Fins configuration (right)

DOI: 10.13009/EUCASS2017-416

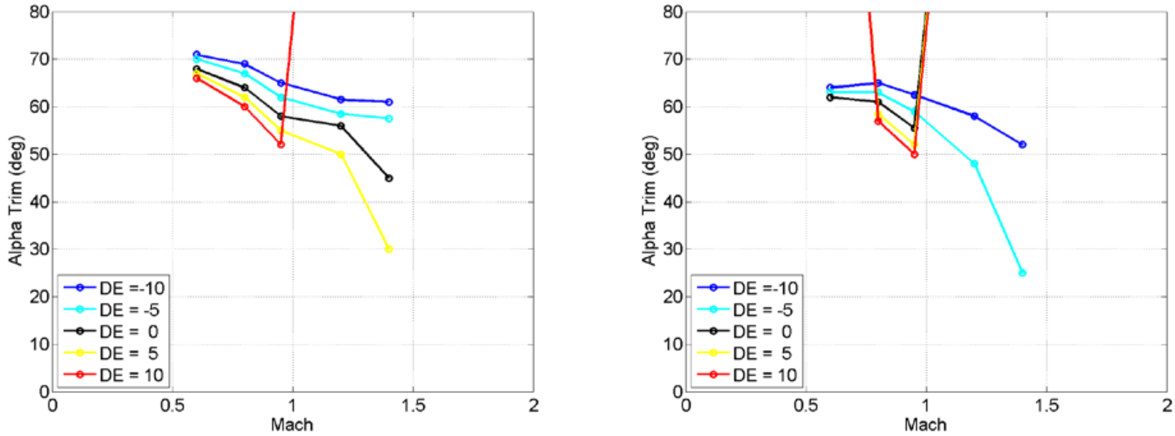

Figure 17: trimmed AoA for IXV configuration (left) and IXV+Fins configuration (right) at constant flap deflection angles

As far as longitudinal aerodynamics is concerned, Figure 16 shows pitching moment coefficient vs. AoA for supersonic to subsonic Mach numbers for the two configurations. Regarding IXV configuration, when Mach number is decreasing, neutral stability zone is beginning to appear at Mach=1.2 between 30 and 50 deg AoA, whereas passing through transonic, a significant pitch-up phenomenon appears, at "low" AoA for Mach=0.95 (30 to 50 deg), and moving up in AoA range when Mach number furtherly decreases (Mach=0.8 and Mach=0.6). The stability AoA range is slightly increasing when Mach number is decreasing, in particular above 50 deg at Mach=0.95, above 55 deg at Mach=0.8 and above 65 deg at Mach=0.6. Natural trim AoA is also slightly increasing when Mach number is decreasing, from 58 deg at Mach=0.95 up to 68 deg at Mach=0.6.

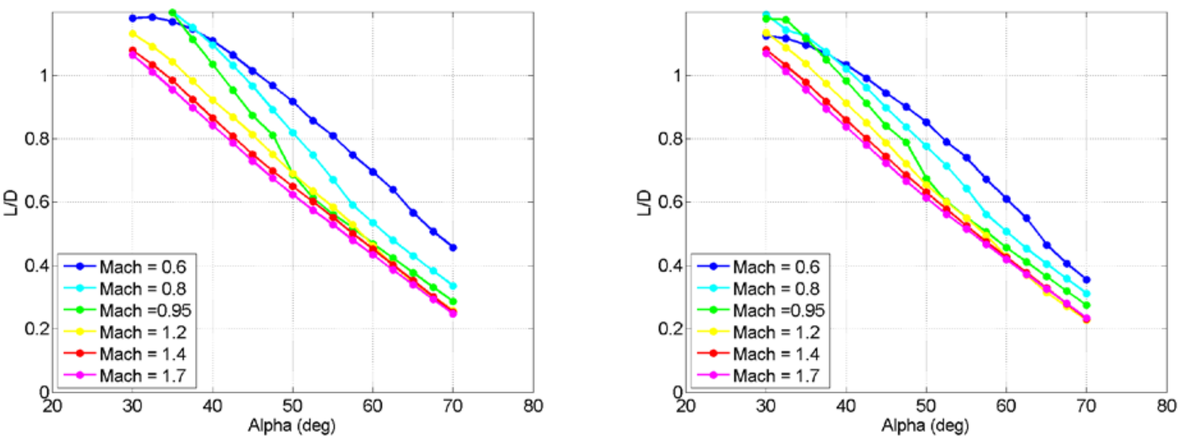

Figure 18: lift-to-drag ratio for IXV configuration (left) and IXV+Fins configuration (right)

Stability AoA ranges for IXV+Fins configuration are quite similar for each Mach numbers. A significant pitch-down effect is observed in supersonic regime, leading to possible trim deflections between -5deg and -10deg, which seems to be not robust enough to ensure longitudinal and lateral trim capability and controllability, because it is close to the actual maximum authorized flap deflections.
This behavior is reflected in trimmed AoA at constant elevon deflections (δ_e=-10÷10 deg) vs. Mach number reported in Figure 17 for the two configurations: trimmed AoA is naturally moving up as Mach number is decreasing in order to stay in the stability range and flap efficiency is decreasing when AoA is increasing. For IXV aeroshape, no trim AoA is reachable for +10deg flap deflection for Mach=1.2 and Mach=1.4, whereas for IXV+FIN aeroshape the only flap deflections that give trimmed conditions through supersonic and subsonic regimes are -5deg and -10deg. Trimmed AoA, when reachable, are around 5deg lower than for IXV as it is.
Figure 18 shows lift-to-drag ratio vs. AoA for supersonic to subsonic Mach numbers. The behavior for the two configurations is quite similar but association with trimmed AoA leads, for IXV aeroshape, to L/D of around 0.7 at Mach=1.4, decreasing to 0.45 at Mach=0.8 at higher AoA whereas for IXV+FIN aeroshape, since trimmed AoAs are in general lower, slightly higher values of L/D ratio are found.

DOI: 10.13009/EUCASS2017-416

Static lateral stability can be estimated through $C_{n\beta}$ coefficient, but more interestingly through the dynamic stability, which is evaluated through "*dynamic $C_{n\beta}$*" which is a combination on $C_{n\beta}$ and $C_{l\beta}$ through the ratio of moments of inertia (I_{zz}/I_{xx}) and the angle of attack (α), i.e.

$$Cn_{\beta}^{Dyn} = Cn_{\beta}.\cos\alpha - \frac{Izz}{Ixx}.Cl_{\beta}.\sin\alpha$$

Figure 19 presents static stability $C_{n\beta}$ for the two configurations: AoA range where $C_{n\beta}$ is positive (stable) is moving up when Mach number is decreasing, but $C_{n\beta}$ remains positive for each Mach number at trimmed AoA. This AoA range of static lateral stability is consistent with longitudinal stability AoA range. Static stability is enhanced in subsonic regime for IXV+Fins, since $C_{n\beta}$ is positive in almost the entire AoA range and for each Mach number.

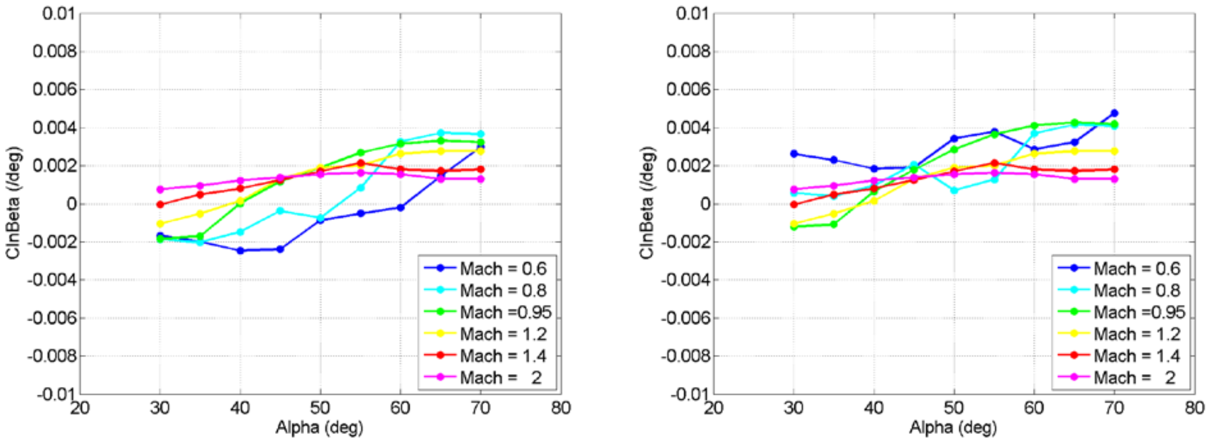

Figure 19: static lateral stability for IXV configuration (left) and IXV+Fins configuration (right)

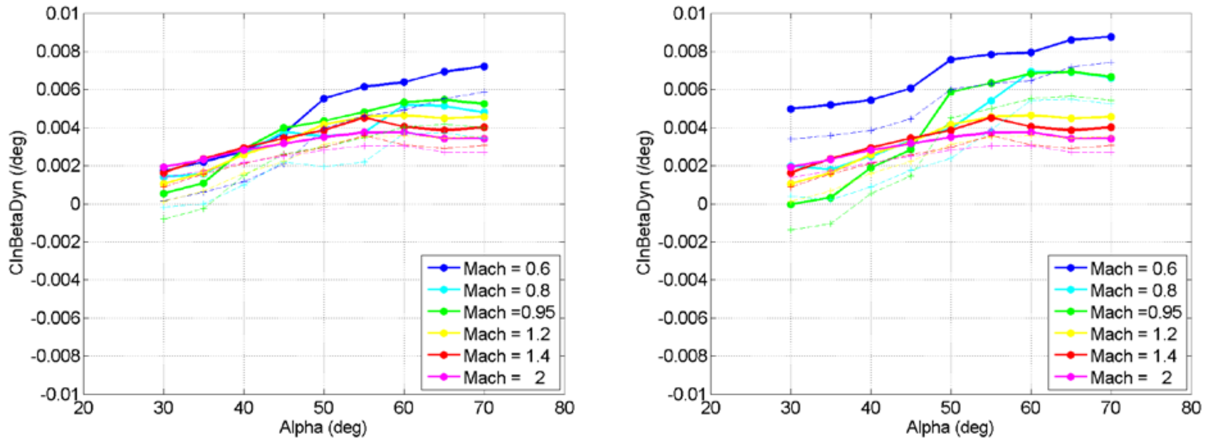

Figure 20: dynamic lateral stability for IXV configuration (left) and IXV+Fins configuration (right)

In Figure 20 the dynamic $C_{n\beta}$ for the two configurations is shown: nominal dynamic $C_{n\beta}$ are presented in solid lines; dashed lines stand for a specific uncertainty case where $C_{n\beta}$ and $C_{l\beta}$ are minimized in absolute value. This shows dynamic lateral stability is always above the usual acceptable threshold fixed at 0.001 in targeted AoA ranges, even when considering uncertainties on $C_{n\beta}$ and $C_{l\beta}$. The same behaviour is also found for IXV+Fins aeroshape, for which dynamic $C_{n\beta}$ is higher in the whole range of Mach numbers and AoA. The dynamic $C_{n\beta}$ is positive in the whole Mach number range, and this is mainly due to the fact that static instabilities ($C_{n\beta}$<0) at subsonic Mach numbers are inhibited by the good dihedral effect ($C_{l\beta}$<0 in all conditions) of the IXV aeroshape.

Lateral controllability is illustrated on Figure 21: results on the left refer to IXV aeroshape and they are obtained for trimmed AoA at δ_e =0 deg for each Mach number, whereas results on the right refer to IXV+FIN aeroshape and they are obtained for trimmed AoA at δ_e =-10deg for each Mach number.

AoS effect and aileron efficiency are both presented as vectors in the (C_n; C_l) diagram; head of each vector is completed with its uncertainty box, as defined in AEDB v6.0. Good controllability is exemplified by perpendicular aileron and AoS vectors, which means that any lateral perturbation can be managed by a combination of a command in aileron deflection and a stabilized AoS. Vectors must not be aligned even when considering uncertainties, and this reflects the condition on the so-called Lateral Control Departure Parameter (LCDP) that measures the static control coupling between the directional axis and the ailerons, i.e.

DOI: 10.13009/EUCASS2017-416

$$LCDP = Cn_{\beta} - \frac{Cn_{\delta a}}{Cl_{\delta a}} . Cl_{\beta} > 0$$

Negative values of LCDP indicate the possibility of roll reversal, that in any case can still be controlled with flap asymmetric deflections.

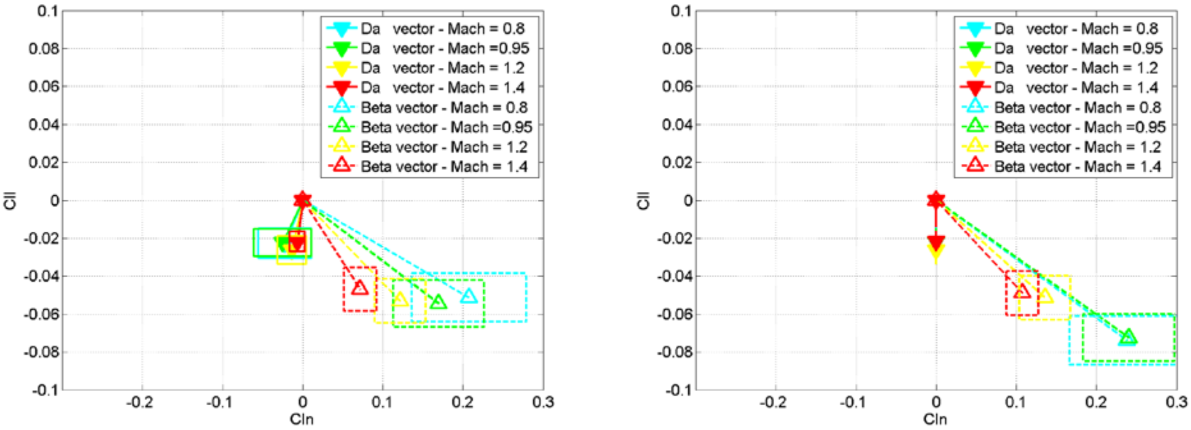

Figure 21: lateral controllability for IXV aeroshape (left, trimmed AoA at δ_e = 0deg) and IXV+Fins aeroshape (right, trimmed AoA at δ_e = -10deg)

Regarding IXV aeroshape, lateral controllability is good for subsonic Mach numbers; it is a bit worse for low supersonic regime but it remains correct since no alignment is observed in vectors even when considering uncertainties. For what concerns IXV+Fins aeroshape, since $C_{n\delta a}$ is assumed to be zero at δ_e =-10deg and -15deg in the AEDB, aileron vectors do not have any coordinate along C_l axis. This is also the reason why no uncertainty box can be seen around head of aileron vector, because uncertainty on aileron efficiency is an uncertainty factor, and $C_{n\delta a}$ remains zero when multiplied by an uncertainty factor.
Because same longitudinal and lateral flap efficiencies are considered for IXV as it is and IXV+Fins in AEDB, lateral controllability for IXV+Fins should be as good as for IXV as it is. The main issue is linked to longitudinal trim around Mach=1.4 that is around -8deg, which significantly reduces available flap capability to dynamically control longitudinal and lateral perturbations.

Conclusions of the Aerodynamic Analysis

According to DAA activities, and on the basis of preliminary FQ analysis performed taking into account IXV MCI properties and aerodynamic uncertainties, the “IXV as it is” vehicle was stable and controllable both in longitudinal and lateral down to M=0.6. A flight strategy following the natural increasing trim angle of attack was proposed by DAA. For what concerns dynamic pitching moment, DAA observed a reduction of dynamic stability for M<0.8 and claimed for further investigation to assess C_{mq} (and C_{mq}+$C_{malphadot}$) behavior at low Mach number.
Concerning CIRA activities focused on the preliminary characterization of the IXV with fins configuration, the modification to the aerodynamic behavior induced by the fins can be summarized in: 1) improved lateral directional stability, 2) reduction of natural trim angle of attack. Preliminary trim-ability analysis performed by CIRA showed, however, that in the low supersonic regime the increase of pitch down moment requires sensibly higher negative elevon deflections.
Considering the conclusions of Section 3, see in particular Table 3, and the above considerations from the aerodynamic point of view, it was confirmed that based on current maturity level, and considering system and cost level impacts, the IXV aeroshape without any modification was selected as baseline.
The comparison between the two configurations and the FQ analyses performed by DEIMOS with the two versions of the aerodynamic database (in the hypothesis of restored MCI, reduced aerodynamic uncertainties and increased flap deflection range) highlighted the possibility to cross transonic and subsonic regime with the “IXV 1:1” configuration.

4.2 Experimental Investigation: INCAS WTT Campaign

At the time of writing, an experimental test campaign at INCAS Trisonic Wind Tunnel (Bucharest, Romania) is being performed, in order to increase the reliability of the updated AEDBs v6.0, to confirm their working hypotheses and to extend the elevon/aileron efficiency evaluation. Operative since 1977, the Trisonic Wind Tunnel is the most advanced

DOI: 10.13009/EUCASS2017-416

facility existing in INCAS experimental platform. The 1.2x1.2m section wind tunnel is of the blowdown type with a speed range from low subsonic (M=0.1) to a maximum supersonic Mach number of 3.5. Transonic Mach numbers are obtained by using a perforated wall transonic test section, to be easily incorporated into the wind tunnel circuit when required. During a run, the control valve is manipulated to give a constant prescribed stagnation pressure (P_0) while the stagnation temperature (T_0) is approximately 20°C. In the subsonic-transonic regime the wind tunnel is able to reproduce any Mach number, while in supersonic regime nozzles are available for nominal Mach numbers 1.1, 1.2, 1.3, 1.4, 1.6, 1.8, 2.0, 2.25, 2.5, 2.75, 3.0, 3.25 and 3.5. The performance map of the tunnel in terms of reservoir pressure, Mach number, Reynolds number and run duration is reported in Figure 22.
Six-component 26-mm diameter TEM balance (sting mounted) has been used for force and moment measurements, with the following load capacity (maximum single component loads): normal force 4670 N, side force 2406 N, axial force 711.5 N; rolling moment 19.2 Nm, pitching moment 148.5 Nm, yawing moment 65.5 Nm. Pressure measurements on model surface are acquired as well as a Schlieren system is used as visualization tool and a special paint can be applied on the model for oil-flow visualization of separated flow regions. The tunnel is equipped with a high speed, high accuracy Data Acquisition System controlled by a PC and having 64 analogic input channels with high accuracy instrumentation amplifiers and low-pass filters. The overall system accuracy (excluding transducers) is better than 0.1%.
The model for "IXV as it is" aeroshape was the IXV model A already used for FOI/STARCS T1500 campaigns in IXV project [3][4][5], see Figure 23, that was provided to INCAS together with related CAD files and test reports of previous campaigns to extract the aerodynamic loads acting on the model for their own verifications. The scale of the model is 1:21, the length without flap is 0.209 m and reference surface is 0.02 m^2. Additionally to the existing tapered flaps (±15 deg, ±10 deg, ±5 deg, 0 deg), a set of left/right tapered flaps with ±20 deg deflection have been manufactured by INCAS, in order to extend the evaluation of the elevon/aileron efficiency. INCAS has also built one STARCS-like longitudinal sting adapter and two bent sting adapters for studying AoS effects, other than the model balance adapter, see Figure 23. The sting operational sweep range is [-14÷24] deg due to safety limitations. Therefore, the positioning of the assembly (model-balance-adapter-sting) with respect to the flow direction is set in such a way to obtain the requested AoA sweep range of [42÷80] deg.

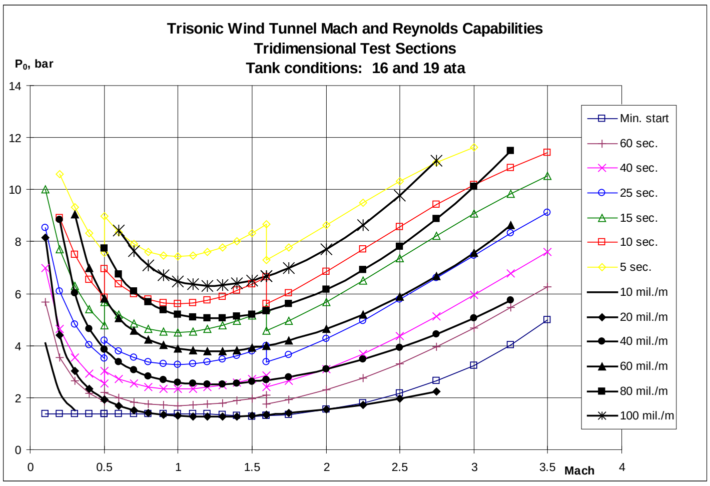

Figure 22: INCAS Trisonic Wind Tunnel performance map

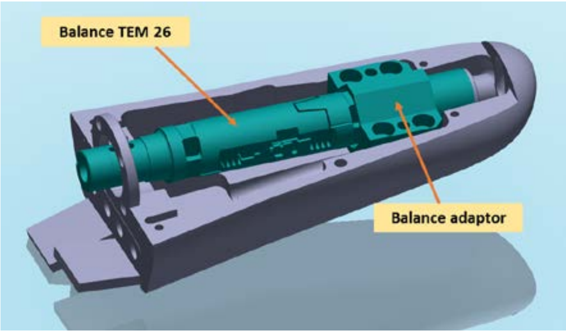

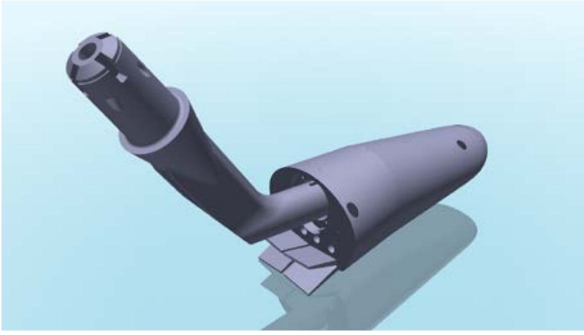

Figure 23: existing model A with balance TEM-26 installed (left) and with longitudinal sting adapter and ±20 deg flaps (right)

DOI: 10.13009/EUCASS2017-416

Unfortunately, the existing IXV model A cannot be used for “IXV with Fins” aeroshape since adding the fins supposes modifications of the lower body. Consequently, a new model has been designed and is being built by INCAS to satisfy modular Space-Rider concept, with two different upper covers with and without fins, see Figure 24.

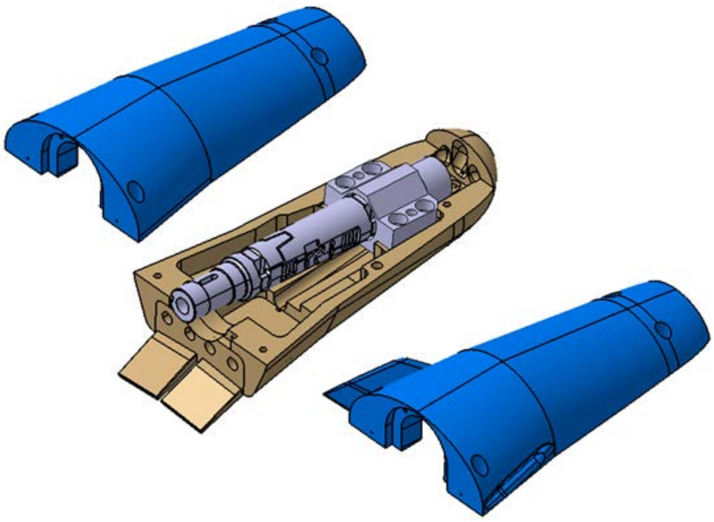

Figure 24: new modular model designed and built by INCAS

With the goal to fix and control the laminar-to-turbulence transition, a tripping device was applied to the models consisting of 80µm carborundum grits in 4mm wide bands, with the same layout used during FOI/STARCS T1500 test campaigns [3][4][5]. The INCAS WTT coverage in terms of Mach number and Reynolds number with respect to Space-Rider available trajectories is shown in Figure 25. A reduction of P_0 at lower Mach numbers has been applied (w.r.t. PRR specification) in order to perform the requested AoA-sweeps in one single run. However, Reynolds number at every Mach number remains larger than in FOI/STARCS T1500 (it is the same only for M=0.6).

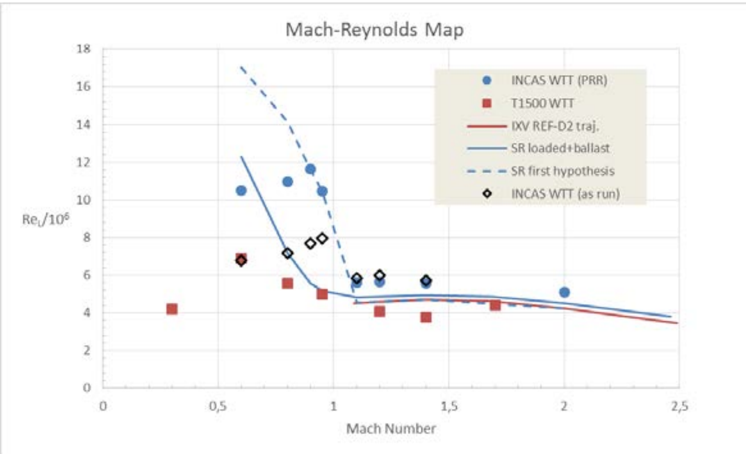

Figure 25: Mach number vs. Reynolds number map

The first WTT campaign (aeroshape “IXV as it is”, model A) is devoted to complete the existing experimental dataset and extend it to lower Mach numbers (i.e. down to Mach=0.6), especially for what concerns elevon and aileron efficiencies. A total of 120 runs is foreseen for Mach numbers 0.6, 0.8, 0.9, 0.95, 1.10, 1.20 and 1.40, with blocks of runs dedicated to the assessment of tripping device effectiveness (by means of oil-paint flow visualizations, with/without tripping devices) and test repeatability (M=0.8, 1.2), study of AoA effect and AoS effect in clean configuration, study of flap efficiency and aileron efficiency with AoS effects, study of coupling between aileron deflection and AoS effect. Cross-checks with FOI/STARCS T1500 measurements are being done when possible. Figure 26 shows some typical results of the oil-paint flow visualizations, in particular for the condition at M=1.2, AoA=56 deg (close to natural trim) and with tripping device applied to the model surface. Traces of vortex structures on leeside and lateral side of the model and skin-friction lines are visible after the test.

DOI: 10.13009/EUCASS2017-416

Figure 26: oil-paint flow visualization, M=1.2, AoA=56 deg, with tripping device

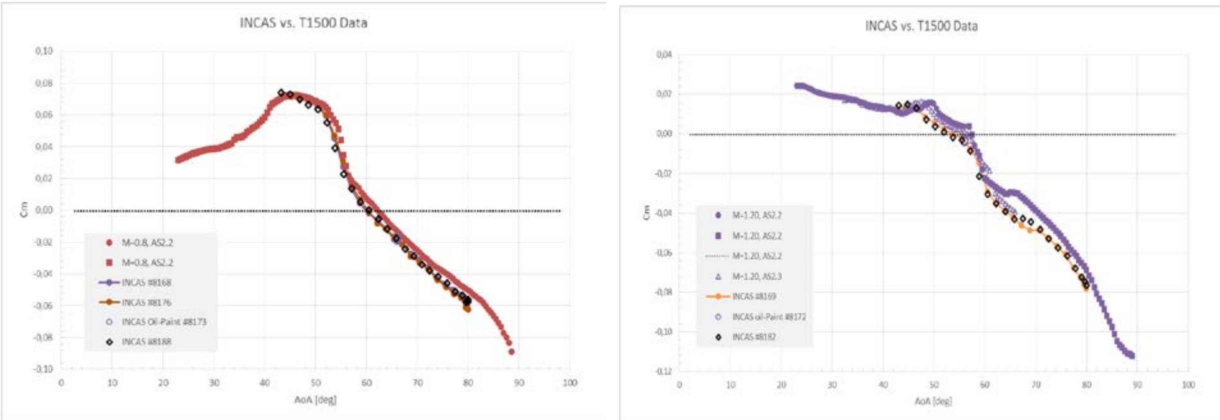

Figure 27: pitching moment coefficient at M=0.8 (left) and M=1.2 (right), INCAS vs. T1500 data

Figure 27 shows the pitching moment coefficient evolution in clean configuration at M=0.8 and M=1.2, with INCAS repeated tests and with the fixed AoA measurement taken during the oil-paint flow visualizations. INCAS test repeatability is good, and the comparison with available T1500 data is acceptable when considering the same aeroshape 2.3. Figure 28-left reports the pitching moment coefficient evolution in clean configuration for all the tested Mach numbers, showing that longitudinal static stability is preserved in the examined AoA range at all Mach numbers, with the exception of M=0.6 for AoA<54 deg. Figure 28-right shows the associated aerodynamic efficiency evolution which decreases almost linearly with increasing AoA, and decreases with Mach number. The conditions of natural trim have been also indicated in the figure, and a difference (1.1÷4.9 deg at same Mach number) has been found out in natural trim AoAs between INCAS and T1500 data (for aeroshape 2.2).

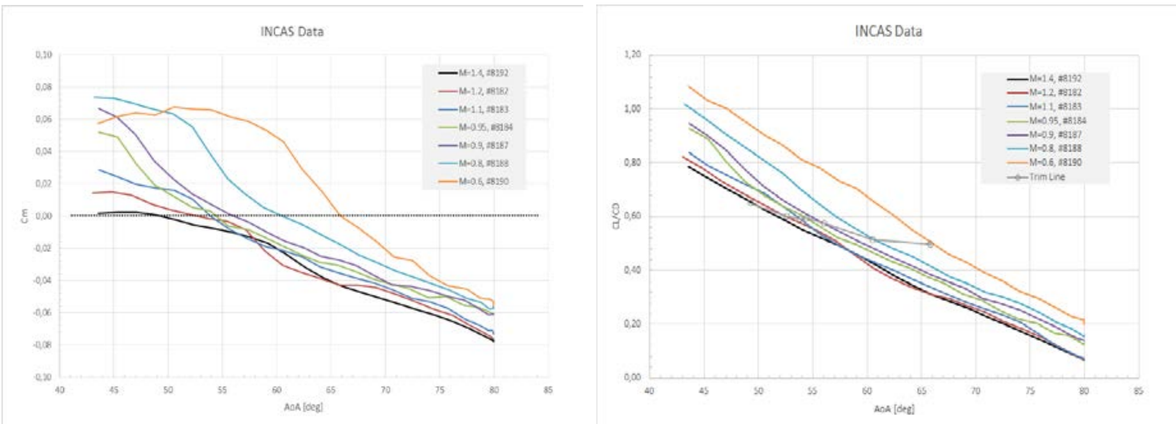

Figure 28: pitching moment coefficient (left) and lift-to-drag ratio (right) in clean configuration, INCAS data

DOI: 10.13009/EUCASS2017-416

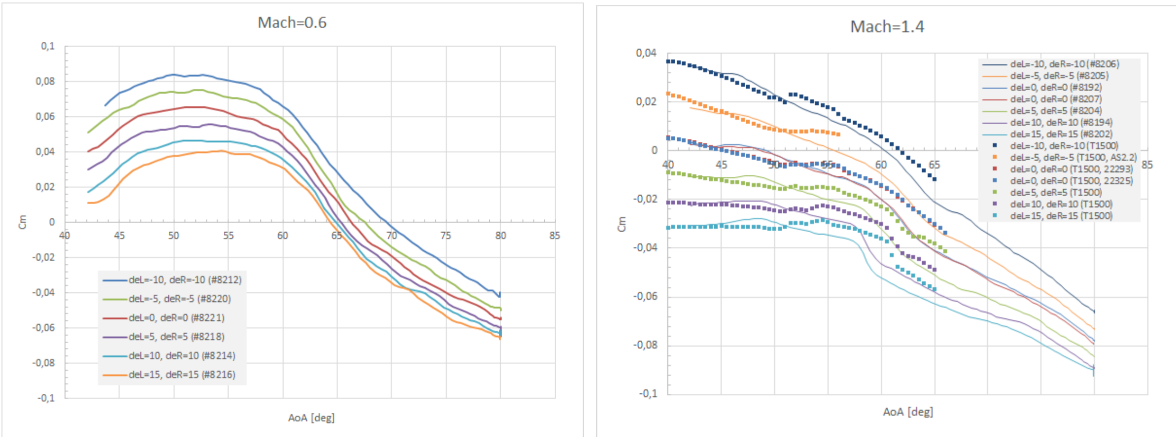

Figure 29: pitching moment coefficient at M=0.6 (left) and M=1.4 (right), elevon efficiency study, INCAS data

Figure 29 depicts the first INCAS data for elevon efficiency investigation (in terms of pitching moment coefficient evolution) at M=0.6 and M=1.4. For M=0.6 tests, whose Reynolds number is 5.95E+6 (P_0≈2.5bar), i.e. roughly 60% of the flight Reynolds number, the trim is possible for the whole investigated range of δ_e (-10÷15 deg) for AoA ranging from 64 to about 69.5 deg. Moreover, a clear longitudinal static stability ($C_{m\alpha}$<0) is observed for AoA>54÷56 deg. For the elevon efficiency study at M=1.4, Reynolds number of tests being 5.75E+6 closer to Space-Rider flight value, while was 3.85E+6 in T1500, the comparison of results reported in Figure 29-right indicates that differences probably are due to the Reynolds effect on the leeward separation, in particular on the critical AoAs at which noticeable gradients of C_m and C_D occur. Measurements data agree very well up to AoA=45 deg for C_m and up to about AoA=50 deg for C_D (not shown). Results also indicate that at M=1.4 trim is possible only for δ_e≤0 deg, and that a clear longitudinal static stability ($C_{m\alpha}$<0) is observed for AoA>46÷49 deg.
The second WTT campaign (aeroshape “IXV with Fins”, new model) is devoted to test the advanced aeroshape with fins, thus creating a first experimental data-package for this configuration at given ranges (the same of IXV as it is) of Mach number, angle of attack and angle of sideslip. A total of 24 runs have been foreseen to study AoA effect and AoS effect in clean configuration, with the extension to M=2 condition not investigated in the first WTT campaign.

4.3 Future Steps

The near future major steps of the aerodynamic activities of Space-Rider program, until the end of Phase B1, are:

- Completion of INCAS WTT Campaign and delivery of experimental data-packages for both configurations, including the correction of aerodynamic data for cavity pressure effects, the experimental aerodynamic uncertainties, the pressure measurements on model surface, and the sting effect correction function (elaborated by INCAS through CFD simulations).
- Update of both AEDBs (“IXV as it is” and “IXV with Fins”) by DAA to increase their reliability, with including:
  - uncertainty model improvement (inputs coming from INCAS WTT data and CFD data produced by DAA, CIRA, FGE, CFSe, University of Rome);
  - dynamic derivatives modeling improvement (inputs from unsteady simulations by CFSe and DAA);
  - Elevon/aileron efficiency with larger tapered flap deflections, i.e. ±15, ±20 deg (inputs coming from INCAS WTT data and FGE CFD simulations for hinge-moment database enrichment).
- Delivery of updated AEDBs to DEIMOS for flight mechanics analysis and final trajectory design loop.

5. Conclusions

In the present paper, the aeroshape trade-off analysis performed during the Phase A of the Space-Rider program has been described in detail. Different classes of aeroshape have been investigated: lifting body, winged body and capsule. Trade-off has relied only on a qualitative evaluation of different aspects (performance, volume, flexibility, development effort), and the IXV-like lifting body concept has been finally selected. Two candidate aeroshape configurations have been selected: the “IXV as it is” and the “IXV with Fins”, a variant of IXV with the addition of a couple of vertical fins.
The extensive aerodynamic investigation performed in Phase A (only numerical) and Phase B1 (experimental and numerical), that however has not been completed yet, together with some preliminary analyses of Flying Qualities, is

DOI: 10.13009/EUCASS2017-416

confirming that the “IXV as it is” aeroshape is stable and controllable both in longitudinal and lateral down to M=0.6. A flight strategy following the natural increasing trim angle of attack has been also proposed by DAA.
Regarding the “IXV with Fins” aeroshape, the modification to the aerodynamic behaviour induced by the fins can be summarized in improved lateral-directional stability and reduction of few degrees of natural trim angle of attack. Preliminary trim-ability analysis performed by CIRA has shown, however, that in the low supersonic regime the increase of pitch down moment requires sensibly higher negative elevon deflections.
Based on current maturity level, and considering system and cost level impacts, the IXV aeroshape without any modification was selected as baseline. The comparison between the two configurations and the still preliminary Flying Qualities analyses performed by DEIMOS with the two versions of the aerodynamic database (in the hypothesis of restored MCI, reduced aerodynamic uncertainties and increased flap deflection range) have highlighted the existence of a possible flight corridor to cross transonic and subsonic regime with the “IXV as it is” configuration.

References

[1] Tumino, G., S. Mancuso, S. Dussy, J.-P. Preaud, G. Rufolo, G. Guidotti, F. Massobrio and A. Denaro. 2016. The Space Rider (Pride) Programme: An Application Driven Approach for the Definition of An Affordable Reusable Space Transportation System. IAC-16-D2.6. *67th International Astronautical Conference (IAC)*, Guadalajara, Mexico, September 26-30, 2016.
[2] Dutheil S. et al. 2014. FLPP IXV Phase D, Aerodynamic Database, SYS-12. IXV-DASS-TNT-1018 Revision 1. DGT134758, issue B, 2 June 2014.
[3] Torngren, L. 2008. Wind Tunnel Test with FLPP IXV Model A in FOI Wind Tunnel T1500, Phase B2-C1. FOI Memo 2382, IXV-FOI-RPT-001, SYS-028B, March 2008.
[4] Sjörs, K. 2010. FLPP IXV Project Phase C2 – FLPP Period 2 Step 1: STARCS T1500 Wind Tunnel Test Report. STARCS10-R-0168, November 2010.
[5] Sjörs, K. 2011. FLPP IXV Project Phase D – FLPP Period 2 Step 2: STARCS Wind Tunnel Test Report. STARCS11-R-0107, March 2011.
[6] Catalano, P., and M. Amato. 2003. An evaluation of RANS turbulence modelling for aerodynamic applications”, *Aerospace Science and Technology Journal*, Vol.7, Issue 7, pp. 493-509.
[7] Hoarau, Y., Pena, D., Vos, J.B., Charbonnier, D., Gehri, A., Braza, M., Deloze, T. and E. Laurendeau. 2016. Recent Developments of the Navier Stokes Multi Block (NSMB) CFD Solver, AIAA 2016-2056. *54th AIAA Aerospace Sciences Meeting, AIAA SciTech Forum*, San Diego, California, USA, 4-8 January 2016. https://doi.org/10.2514/6.2016-2056
[8] Chalot, F., Mallet, M., and M. Ravachol. 1994. A Comprehensive Finite Element Navier-Stokes Solver for Low- and High-Speed Aircraft Design, AIAA-94-0814. *AIAA 32nd Aerospace Sciences Meeting*, Reno, Nevada, 10-13 January 1994.
[9] Bowcutt, K.G. 2008. Aerodynamic Design and Analysis. Hypersonic Educational Initiative, NASA, June 2008.
[10] Barua, P., Sousa, T., and D. Scholz. 2015. Empennage Statistics and Sizing Methods for Dorsal Fins. University of Hamburg, AERO_TN_TailSizing_13-04-2015.
[11] Hettema, A.P. 2015. Vertical Tail Design. Development of a Rapid Aerodynamic Analysis Method. Master of Science in Aerospace Engineering, TU Delft, 251#15#MT#DAR_FPP, May 2015.